

# OFDM With Index Modulation Using Coordinate Interleaving

Ertuğrul Başar, *Member, IEEE*

**Abstract**—Orthogonal frequency division multiplexing with index modulation (OFDM-IM), which uses the indices of the active subcarriers to transmit data, is a recently proposed multicarrier transmission technique. In this letter, we propose coordinate interleaved OFDM-IM (CI-OFDM-IM) by combining OFDM-IM and space-time block codes with coordinate interleaving. In this scheme, the real and imaginary parts of the data symbols are transmitted over different active subcarriers to achieve an additional diversity gain. The average bit error probability (ABEP) of the proposed scheme is derived and its superiority over the reference systems is shown via computer simulations.

**Index Terms**—OFDM, coordinate interleaved orthogonal designs (CIODs), index modulation, pairwise error probability.

## I. INTRODUCTION

ORTHOGONAL frequency division multiplexing (OFDM) is a highly popular multicarrier transmission technique and has been included in many wireless communications standards due to its robustness to the intersymbol interference. OFDM with index modulation (OFDM-IM) is a novel OFDM scheme which transmits the information not only by the  $M$ -ary signal constellations, but also by the indices of the subcarriers, which are activated according to the corresponding information bits [1]. Compared to the classical OFDM, OFDM-IM provides an interesting trade-off between performance and spectral efficiency by the adjustment of the number of active subcarriers in the system.

Index modulation techniques for OFDM have attracted significant attention from researchers, and have been investigated in some very recent studies [2]–[5]. In [2] subcarrier level block interleaving is introduced for OFDM-IM to improve its error performance. A tight approximation for the bit error rate (BER) of OFDM-IM is presented in [3]. In [4], the spectral efficiency of OFDM-IM is improved by selecting the active subcarriers in a more flexible way. The problem of selecting the optimal number of active subcarriers for the OFDM-IM scheme is investigated in [5]. The aforementioned studies generally focused on improving the error performance and/or spectral efficiency of the OFDM-IM scheme; however, to the best of our knowledge, the diversity potential of the OFDM-IM has not been explored in the literature yet.

In this letter, we combine OFDM-IM and space-time block codes with coordinate interleaving to achieve an additional diversity gain. In the proposed *coordinate interleaved OFDM-IM* (CI-OFDM-IM) scheme, the real and imaginary parts of the

Manuscript received February 27, 2015; revised April 12, 2015; accepted April 13, 2015. Date of publication April 15, 2015; date of current version August 20, 2015. The associate editor coordinating the review of this paper and approving it for publication was L. Lampe.

The author is with the Faculty of Electrical and Electronics Engineering, Istanbul Technical University, Istanbul 34469, Turkey (e-mail: basarer@itu.edu.tr).

Digital Object Identifier 10.1109/LWC.2015.2423282

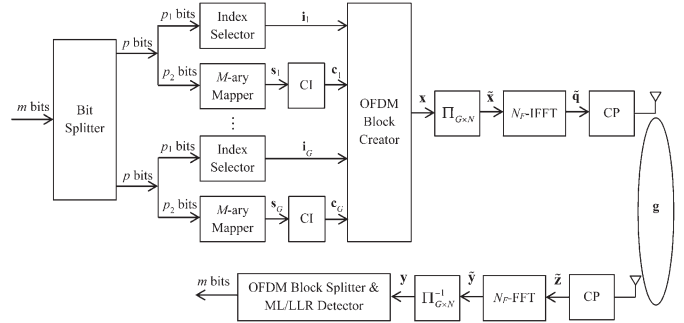


Fig. 1. Transceiver structure of the CI-OFDM-IM scheme.

complex data symbols are transmitted over different active subcarriers of the OFDM-IM scheme. Transceiver structure of the proposed scheme is constructed and its average bit error probability (ABEP) upper bound is derived. It is shown via computer simulations that CI-OFDM-IM provides significantly better error performance than the OFDM-IM scheme and the classical OFDM due to its higher diversity gain.

The rest of the letter is organized as follows. In Section II, the system model of CI-OFDM-IM is given. Performance analysis and optimization of the CI-OFDM-IM scheme are presented in Section III. Simulation results are provided in Section IV. Finally, conclusions are given in Section V.<sup>1</sup>

## II. SYSTEM MODEL OF CI-OFDM-IM

The block diagram of the CI-OFDM-IM scheme is given in Fig. 1. For the transmission of each OFDM block, a total of  $m$  information bits enter the transmitter of the CI-OFDM-IM scheme. These bits are split into  $G$  groups each containing  $p = p_1 + p_2$  bits, which are used to form OFDM subblocks of length  $N = N_F/G$ , where  $N_F$  is the size of the fast Fourier transform (FFT). For each subblock  $g$  ( $g = 1, 2, \dots, G$ ), only  $K$  out of  $N$  available subcarriers are activated by the index selector according to the corresponding  $p_1 = \lfloor \log_2(C(N, K)) \rfloor$  bits, while the remaining  $N - K$  subcarriers are inactive. For each subblock  $g$ , the selected active subcarrier indices are given by<sup>2</sup>

$$\mathbf{i}_g = [i_1 \quad i_2 \quad \dots \quad i_K]^T, \quad g = 1, 2, \dots, G \quad (1)$$

<sup>1</sup>Notation: Bold, lowercase and capital letters are used for column vectors and matrices, respectively.  $(\cdot)^T$  and  $(\cdot)^H$  denote transposition and Hermitian transposition, respectively.  $\det(\mathbf{A})$  and  $\text{rank}(\mathbf{A})$  denote the determinant and rank of  $\mathbf{A}$ , respectively.  $\mathbf{I}_{N \times N}$  is the identity matrix with dimensions  $N$ .  $\|\cdot\|$  stands for the Euclidean norm.  $E\{\cdot\}$  stands for expectation. The probability density function (p.d.f.) of a random variable (r.v.)  $X$  is denoted by  $p(X)$ .  $X \sim \mathcal{CN}(0, \sigma_X^2)$  represents the distribution of a circularly symmetric complex Gaussian r.v.  $X$  with variance  $\sigma_X^2$ .  $Q(\cdot)$  denotes the tail probability of the standard Gaussian distribution.  $C(N, K)$  stands for the binomial coefficient and  $\lfloor \cdot \rfloor$  is the floor function.  $\mathcal{S}$  and  $\mathcal{S}^\theta$  denote  $M$ -QAM and rotated  $M$ -QAM signal constellations, respectively.  $\mathbb{C}$  denotes the ring of complex numbers and  $j$  is the unit imaginary number  $j = \sqrt{-1}$ .

<sup>2</sup>Please note that we dropped subscript  $g$  for the elements of  $\mathbf{i}_g$  for the clarity of the presentation.

TABLE I  
A LOOK-UP TABLE EXAMPLE FOR  $N = 4$ ,  $K = 2$ , AND  $p_1 = 2$

$p_1$ -bits	Indices ( $\mathbf{i}_g^T$ )
[0 0]	[1 3]
[0 1]	[2 4]
[1 0]	[1 4]
[1 1]	[2 3]

where  $i_k \in \{1, 2, \dots, N\}$  for  $k = 1, 2, \dots, K$ . This subcarrier index selection procedure can be performed either using a look-up table for smaller  $N$  and  $K$  values or using a one-to-one mapper based on combinatorial method, which maps natural numbers to  $K$ -combinations [1]. In Table I, an index selection example is provided for the look-up table method.

For each subblock, the remaining  $p_2 = K(\log_2(M))$  bits of the  $p$ -bit input bit sequence are mapped onto the  $M$ -ary signal constellation in order to determine the data symbols that are transmitted over the active subcarriers. For the CI-OFDM-IM scheme, rotated square  $M$ -ary quadrature amplitude modulation ( $M$ -QAM) constellations are considered. Assume that a square  $M$ -QAM constellation with signal points  $s = s^R + js^I \in \mathcal{S}$  is rotated by an angle of  $\theta$ . In this case, the rotated signal constellation symbols become  $se^{j\theta} \in \mathcal{S}^\theta$ . Constellation rotation [6] is an integral part of a transmission scheme based on coordinate interleaving to achieve diversity gain. For each subblock  $g$ , at the output of the  $M$ -ary mapper,  $K$  complex data symbols are obtained as  $\mathbf{s}_g = [s_1 \ s_2 \ \dots \ s_K]^T$ , where  $s_k \in \mathcal{S}^\theta$  for  $k = 1, 2, \dots, K$ . We assume that  $E\{\mathbf{s}_g^H \mathbf{s}_g\} = K$ , i.e., the signal constellation is normalized to have unit average power. For  $K$  being an even number, coordinate interleaving (CI) block processes the input symbol vector  $\mathbf{s}_g$  and transforms it to

$$\mathbf{c}_g = \begin{bmatrix} c_1 \\ c_2 \\ c_3 \\ c_4 \\ \vdots \\ c_{K-1} \\ c_K \end{bmatrix} = \begin{bmatrix} s_1^R + js_2^I \\ s_2^R + js_1^I \\ s_3^R + js_4^I \\ s_4^R + js_3^I \\ \vdots \\ s_{K-1}^R + js_K^I \\ s_K^R + js_{K-1}^I \end{bmatrix} \quad (2)$$

for  $g = 1, 2, \dots, G$ . In our scheme, the elements of  $\mathbf{c}_g$  are transmitted over the  $K$  active subcarriers, whose indices are given in  $\mathbf{i}_g$  in the respective order for each subblock  $g$ . As seen from (2), transmission model of the CI-OFDM-IM scheme is based on the coordinate interleaved orthogonal design (CIOD) for two transmit antennas, which is an application of the signal-space diversity for multiple antenna systems, and can be represented by the following  $2 \times 2$  transmission matrix [6]

$$\begin{bmatrix} s_1^R + js_2^I & 0 \\ 0 & s_2^R + js_1^I \end{bmatrix} \quad (3)$$

where  $s_1, s_2 \in \mathcal{S}^\theta$  and the columns and the rows of (3) correspond to time slots and transmit antennas, respectively.

The OFDM block creator creates all of the subblocks by considering  $\mathbf{i}_g$  and  $\mathbf{c}_g$  for all  $g$  before forming the main OFDM block  $\mathbf{x} = [\mathbf{x}_1^T \ \mathbf{x}_2^T \ \dots \ \mathbf{x}_G^T]^T$ . Compared to the OFDM-IM scheme in which the  $K$  symbols in  $\mathbf{s}_g = [s_1 s_2 \dots s_K]^T$  are transmitted over the selected  $K$  active indices in  $\mathbf{i}_g$  for each subblock, in the CI-OFDM-IM scheme, the real and imaginary

TABLE II  
SUBBLOCK STRUCTURES OF OFDM-IM AND CI-OFDM-IM SCHEMES FOR  $N = 4$  AND  $K = 2$  (LOOK-UP TABLE METHOD)

$p_1$ -bits	OFDM-IM Subblocks ( $\mathbf{x}_g^T$ )	CI-OFDM-IM Subblocks ( $\mathbf{x}_g^T$ )
[0 0]	$[s_1 \ 0 \ s_2 \ 0]$	$[s_1^R + js_2^I \ 0 \ s_2^R + js_1^I \ 0]$
[0 1]	$[0 \ s_1 \ 0 \ s_2]$	$[0 \ s_1^R + js_2^I \ 0 \ s_2^R + js_1^I]$
[1 0]	$[s_1 \ 0 \ 0 \ s_2]$	$[s_1^R + js_2^I \ 0 \ 0 \ s_2^R + js_1^I]$
[1 1]	$[0 \ s_1 \ s_2 \ 0]$	$[0 \ s_1^R + js_2^I \ s_2^R + js_1^I \ 0]$

parts of the each complex information symbol are separated and they are transmitted over two different active subcarriers using coordinate interleaving principle to achieve an additional diversity gain. In Table II, subblock structures of the OFDM-IM and CI-OFDM-IM schemes are provided for the look-up table mapping example given in Table I.

After the formation of the main OFDM block  $\mathbf{x}$  by the concatenation of  $G$  subblocks, a  $G \times N$  block interleaver ( $\Pi_{G \times N}$ ) is employed in order to transmit the elements of the subblocks from uncorrelated channels as in [2]. This block interleaver fills a  $G \times N$  matrix row by row with the elements of  $\mathbf{x}$  and sends the contents of this matrix column by column to form the block interleaved OFDM frame  $\tilde{\mathbf{x}}$ .

As seen from Fig. 1, after block interleaving, the resulting OFDM frame  $\tilde{\mathbf{x}}$  is processed by the inverse FFT (IFFT) to obtain  $\tilde{\mathbf{q}}$ . We assume that IFFT operation satisfies  $E\{\tilde{\mathbf{q}}^H \tilde{\mathbf{q}}\} = N_F$ . After the addition of a cyclic prefix (CP) of length  $C_p$ , parallel-to-serial and digital-to-analog conversions, the resulting signal is sent through a  $L$ -tap frequency selective Rayleigh fading channel represented by  $\mathbf{g}$  in the time-domain, whose elements follow  $\mathcal{CN}(0, \frac{1}{L})$  distribution. Assuming the wireless channel remains constant during the transmission of an OFDM block and  $C_p > L$ , after the FFT operation at the receiver, the equivalent input-output relationship of the CI-OFDM-IM scheme in the frequency domain can be written as

$$\tilde{\mathbf{y}} = \mathbf{h}^T \tilde{\mathbf{x}} + \mathbf{w} \quad (4)$$

where  $\tilde{\mathbf{y}}$ ,  $\mathbf{h}$  and  $\mathbf{w}$  are the received signal, channel coefficients and noise vectors in the frequency domain, respectively, all having  $N_F \times 1$  dimensions. The elements of  $\mathbf{h}$  and  $\mathbf{w}$  follow  $\mathcal{CN}(0, 1)$  and  $\mathcal{CN}(0, N_{0,F})$  distributions, respectively, where  $N_{0,F}$  is the noise variance in the frequency-domain, which is related to the noise variance in the time-domain as  $N_{0,T} = (N_F/(KG))N_{0,F}$ . The signal-to-noise ratio (SNR) is defined as  $\rho = E_b/N_{0,T}$  where  $E_b = (N_F + C_p)/m$  is the average transmitted energy per bit. The spectral efficiency of the CI-OFDM-IM scheme is the same as that of OFDM-IM and given by  $m/(N_F + C_p)$  [bits/s/Hz].

Before detection at the receiver, the corresponding block deinterleaver ( $\Pi_{G \times N}^{-1} = \Pi_{N \times G}$ ) is employed to obtain

$$\mathbf{y} = \check{\mathbf{h}}^T \mathbf{x} + \check{\mathbf{w}} = \mathbf{X} \check{\mathbf{h}} + \check{\mathbf{w}} \quad (5)$$

where  $\mathbf{X} = \text{diag}(\mathbf{x}) \in \mathbb{C}^{N_F \times N_F}$ , and  $\check{\mathbf{h}}$  and  $\check{\mathbf{w}}$  are deinterleaved (or interleaved with  $\Pi_{N \times G}$ ) versions of  $\mathbf{h}$  and  $\mathbf{w}$ , respectively. As reported in [1], the elements of  $\mathbf{h}$  are highly correlated with the correlation matrix  $\mathbf{K} = E\{\mathbf{h}\mathbf{h}^H\}$ , while using a block interleaver, it is observed that  $\check{\mathbf{K}} = E\{\check{\mathbf{h}}\check{\mathbf{h}}^H\} \approx \mathbf{I}_{N_F}$ , for practical  $N_F$  values, such as  $N_F = 128, 256$ , etc.

*i) ML Detection:* The maximum likelihood (ML) detection of the CI-OFDM-IM scheme is performed after splitting the received OFDM block into  $G$  subblocks to determine the corresponding active indices and data symbols for each of these subblocks by considering  $\mathbf{y} = [\mathbf{y}_1^T \mathbf{y}_2^T \cdots \mathbf{y}_G^T]^T$ ,  $\check{\mathbf{h}} = [\check{\mathbf{h}}_1^T \check{\mathbf{h}}_2^T \cdots \check{\mathbf{h}}_G^T]^T$  and  $\check{\mathbf{w}} = [\check{\mathbf{w}}_1^T \check{\mathbf{w}}_2^T \cdots \check{\mathbf{w}}_G^T]^T$ . For this purpose, (5) can be decomposed for each subblock  $g \in \{1, 2, \dots, G\}$  as

$$\mathbf{y}_g = \mathbf{X}_g \check{\mathbf{h}}_g + \check{\mathbf{w}}_g \quad (6)$$

where  $\mathbf{X}_g = \text{diag}(\mathbf{x}_g) \in \mathbb{C}^{N \times N}$ . The ML detector of the CI-OFDM-IM scheme makes a joint decision on the active indices and data symbols for each subblock  $g$  using

$$\hat{\mathbf{X}}_g = \arg \min_{\mathbf{x}_g} \left\| \mathbf{y}_g - \mathbf{X}_g \check{\mathbf{h}}_g \right\|^2. \quad (7)$$

Since  $\mathbf{X}_g$  has  $RM^K$  different realizations (due to  $R = 2^{p_1}$  active index combinations and  $K$  data symbols), the number of metric calculations performed in (7) is equal to  $RM^K$ . However, using single-symbol ML decoding property of CIODs, this number can be reduced as follows. Without loss of generality, for a given subblock  $g$ , (6) can be rewritten as

$$\begin{bmatrix} y_1 \\ y_2 \\ \vdots \\ y_N \end{bmatrix} = \begin{bmatrix} x_1 & & & \\ & x_2 & & \\ & & \ddots & \\ & & & x_N \end{bmatrix} \begin{bmatrix} \check{h}_1 \\ \check{h}_2 \\ \vdots \\ \check{h}_N \end{bmatrix} + \begin{bmatrix} \check{w}_1 \\ \check{w}_2 \\ \vdots \\ \check{w}_N \end{bmatrix} \quad (8)$$

where due to the index selection, only  $K$  elements of  $\mathbf{X}_g$  are nonzero,  $x_{i_k} = c_k$ ,  $k = 1, 2, \dots, K$ . For each realization of  $\mathbf{i}_g = [i_1 i_2 \cdots i_K]^T$ , which is denoted by  $(\mathbf{i}_g)_r$ ,  $r = 1, 2, \dots, R$  for convenience, the ML detector obtains  $K/2$  equivalent channel models for each pair of the symbols  $(s_a, s_b)$  in  $\mathbf{s}_g$  as

$$\begin{bmatrix} y_{i_a}^R \\ y_{i_a}^I \\ y_{i_b}^R \\ y_{i_b}^I \end{bmatrix}_r = \begin{bmatrix} \check{h}_{i_a}^R & 0 & 0 & -\check{h}_{i_a}^I \\ \check{h}_{i_a}^I & 0 & 0 & \check{h}_{i_a}^R \\ 0 & -\check{h}_{i_b}^I & \check{h}_{i_b}^R & 0 \\ 0 & \check{h}_{i_b}^R & \check{h}_{i_b}^I & 0 \end{bmatrix}_r \times \begin{bmatrix} s_a^R \\ s_a^I \\ s_b^R \\ s_b^I \end{bmatrix} + \begin{bmatrix} \check{w}_{i_a}^R \\ \check{w}_{i_a}^I \\ \check{w}_{i_b}^R \\ \check{w}_{i_b}^I \end{bmatrix}_r$$

$$(\bar{\mathbf{y}}_l)_r = (\bar{\mathbf{H}}_l)_r \bar{\mathbf{s}}_l + (\bar{\mathbf{w}}_l)_r = [(\bar{\mathbf{H}}_{l,1})_r \quad (\bar{\mathbf{H}}_{l,2})_r] \bar{\mathbf{s}}_l + (\bar{\mathbf{w}}_l)_r \quad (9)$$

for  $l = 1, 2, \dots, K/2$ , where  $a = 2l - 1$  and  $b = 2l$ . Due to the orthogonality of the columns of  $(\bar{\mathbf{H}}_l)_r$ , which allows single symbol ML decoding [7], the ML receiver calculates the following total ML metric for each active subcarrier index combination  $r \in \{1, 2, \dots, R\}$  as

$$D(r) = \sum_{l=1}^{K/2} \left( \min_{s_a \in \mathcal{S}^\theta} \left\| (\bar{\mathbf{y}}_l)_r - (\bar{\mathbf{H}}_{l,1})_r \begin{bmatrix} s_a^R \\ s_a^I \end{bmatrix} \right\|^2 + \min_{s_b \in \mathcal{S}^\theta} \left\| (\bar{\mathbf{y}}_l)_r - (\bar{\mathbf{H}}_{l,2})_r \begin{bmatrix} s_b^R \\ s_b^I \end{bmatrix} \right\|^2 \right). \quad (10)$$

Finally, the ML receiver makes a decision onto the active subcarrier indices and corresponding data symbols from  $\hat{r} = \arg \min_r D(r)$ ,  $\hat{s}_a = \arg \min_{s_a} \left\| (\bar{\mathbf{y}}_l)_{\hat{r}} - (\bar{\mathbf{H}}_{l,1})_{\hat{r}} \begin{bmatrix} s_a^R \\ s_a^I \end{bmatrix} \right\|^2$  and  $\hat{s}_b = \arg \min_{s_b} \left\| (\bar{\mathbf{y}}_l)_{\hat{r}} - (\bar{\mathbf{H}}_{l,2})_{\hat{r}} \begin{bmatrix} s_b^R \\ s_b^I \end{bmatrix} \right\|^2$ , for  $l = 1, 2,$

$\dots, K/2$ ,  $a = 2l - 1$ ,  $b = 2l$ . As seen from (10), the total number of metric calculations is reduced from  $RM^K$  to  $RMK$ , which linearly increases with  $K$ .

*ii) LLR Detection:* The LLR detector [1] of the CI-OFDM-IM scheme does not search for all possible active index combinations as the ML detector, and it is employed for higher  $N$  and  $K$  values. On the other hand, for each subblock, it decides to the active indices by calculating

$$\lambda_n = \frac{|y_n|^2}{N_{0,F}} + \ln \left( \sum_c \exp \left( -\frac{1}{N_{0,F}} |y_n - \check{h}_n c|^2 \right) \right) \quad (11)$$

for  $n = 1, 2, \dots, N$ , where  $c$  is the element of the  $M^2$ -ary constellation created by the selection of two symbols such as  $(s_1, s_2) \in \mathcal{S}^\theta$ , and forming  $c = s_1^R + js_2^I$ . In other words, (11) calculates the likelihood ratio for the  $n$ th sub carrier considering the fact that it can be either zero or non-zero with a coordinate interleaved symbol ( $c$ ) transmitted over it. After the calculation of  $N$  LLR values for each subblock, the receiver decides on  $K$  active indices out of them having maximum LLR values. Once the active indices  $(\hat{r})$  are found, the corresponding data symbols  $(\hat{s}_1, \hat{s}_2, \dots, \hat{s}_K)$  on these active subcarriers can be determined using the same decision rules as those of  $\hat{s}_a$  and  $\hat{s}_b$  for the ML detector.

### III. PERFORMANCE ANALYSIS AND OPTIMIZATION OF CI-OFDM-IM

In this section, we analytically evaluate the ABEP of the CI-OFDM-IM scheme for the ML detection; however, the provided results can be assumed to be valid for the LLR detection which is a near-ML detection technique [1]. Since  $\check{\mathbf{K}} \approx \mathbf{I}_{N_F}$ , it is sufficient to investigate the pair wise error probability (PEP) events within a single subblock to determine the overall system performance.

For the channel model given in (6), if  $\mathbf{X}_g$  is transmitted and it is erroneously detected as  $\hat{\mathbf{X}}_g$ , the well-known conditional PEP (CPEP) expression can be written as [8]

$$P(\mathbf{X}_g \rightarrow \hat{\mathbf{X}}_g | \check{\mathbf{h}}_g) = Q \left( \sqrt{\Gamma / (2N_{0,F})} \right) \quad (12)$$

where  $\Gamma = \|(\mathbf{X}_g - \hat{\mathbf{X}}_g) \check{\mathbf{h}}_g\|^2$ . Using the alternative form of the  $Q$ -function [8], and integrating (12) over  $p(\Gamma)$ , we obtain the unconditional PEP (UPEP) as

$$P(\mathbf{X}_g \rightarrow \hat{\mathbf{X}}_g) = \frac{1}{\pi} \int_0^{\pi/2} M_\Gamma \left( -\frac{1}{4 \sin^2 \phi} \right) d\phi. \quad (13)$$

Expressing  $\Gamma$  in the quadratic form as  $\Gamma = \check{\mathbf{h}}_g^H \mathbf{Q} \check{\mathbf{h}}_g$ , where  $\mathbf{Q} = (\mathbf{X}_g - \hat{\mathbf{X}}_g)^H (\mathbf{X}_g - \hat{\mathbf{X}}_g)$ , its moment generating function can be calculated from [8] as  $M_\Gamma(t) = [\det(\mathbf{I}_N - t\mathbf{Q})]^{-1} = [\prod_{i=1}^q (1 - t\lambda_i)]^{-1}$ , where  $q = \text{rank}(\mathbf{Q})$  with non-zero eigenvalues of  $\mathbf{Q}$  being  $\lambda_i$ ,  $i = 1, 2, \dots, q$  for  $q \leq N$ . Substituting  $M_\Gamma(t)$  in (13), we obtain

$$P(\mathbf{X}_g \rightarrow \hat{\mathbf{X}}_g) = \frac{1}{\pi} \int_0^{\pi/2} \prod_{i=1}^q \left( \frac{\sin^2 \phi}{\sin^2 \phi + \frac{\lambda_i}{4N_{0,F}}} \right) d\phi \quad (14)$$

which has a closed form solution in Appendix (5.A) of [8]. After the evaluation of the UPEP, the ABEP of the CI-OFDM-IM

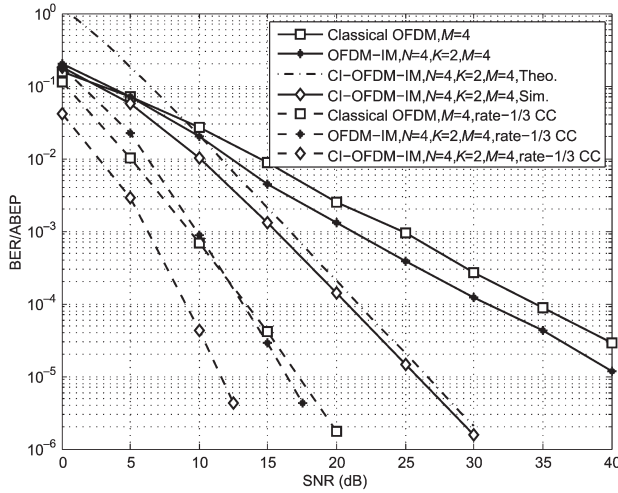


Fig. 2. Uncoded/coded performance of OFDM, OFDM-IM, and CI-OFDM-IM.

scheme can be obtained by the asymptotically tight union upper bound as  $P_b \leq (1/(pn_{\mathbf{x}_g})) \sum_{\mathbf{X}_g} \sum_{\hat{\mathbf{X}}_g} P(\mathbf{X}_g \rightarrow \hat{\mathbf{X}}_g) \times e(\mathbf{X}_g, \hat{\mathbf{X}}_g)$ , where  $n_{\mathbf{x}_g} = RM^K$  is the total number of possible realizations of  $\mathbf{X}_g$  and  $e(\mathbf{X}_g, \hat{\mathbf{X}}_g)$  is the number of bit errors for the corresponding PEP event ( $\mathbf{X}_g \rightarrow \hat{\mathbf{X}}_g$ ).

It is observed from (14) that the diversity order of the CI-OFDM-IM scheme is equal to  $\min_{\mathbf{X}_g, \hat{\mathbf{X}}_g} (q) = 2$  for  $\mathbf{X}_g \neq \hat{\mathbf{X}}_g$ , when a non-zero constellation rotation angle  $\theta$  is chosen. On the other hand, the value of  $\theta$  directly affects  $\lambda_i, i = 1, 2, \dots, q$  and as a result the ABEP. For the optimization of  $\theta$ , we focus on the worst case PEP events which give  $q = 2$ , and obtain the optimum  $\theta$  value as  $\theta_{\text{opt}} = \arg \max_{\theta} \delta_{\min}$ , where  $\delta_{\min}$  is the minimum coding gain distance (CGD), which is an important parameter for the minimization of (14) and defined as  $\delta_{\min} = \min_{\mathbf{X}_g, \hat{\mathbf{X}}_g} \prod_{i=1}^q \lambda_i$ . Since performing an exhaustive search over all possible  $(\mathbf{X}_g, \hat{\mathbf{X}}_g)$  pairs becomes impractical for higher  $N$  and  $K$  values, without loss of generality, we calculate  $\delta_{\min}$  for  $\mathbf{X}_g \in \{\mathbf{X}^1\}$  and  $\hat{\mathbf{X}}_g \in \{\mathbf{X}^1, \mathbf{X}^2\}$ , where  $\mathbf{X}^1 = \text{diag}[(c_1 \ 0 \ c_2 \ 0)]^T$  and  $\mathbf{X}^2 = \text{diag}[(c_1 \ 0 \ 0 \ c_2)]^T$  for  $c_1 = s_1^R + js_2^I, c_2 = s_2^R + js_1^I$  and  $N = 4, K = 2$ , which corresponds to the following two generic PEP events that give  $q = 2$ :  $i)$  ( $\mathbf{X}^1 \rightarrow \mathbf{X}^1$ ): correct active indices, erroneous data symbols,  $ii)$  ( $\mathbf{X}^1 \rightarrow \mathbf{X}^2$ ): one erroneous active index, correct/erroneous data symbols. The following  $\theta_{\text{opt}}$  values are obtained with computer search for 4-, 16-, and 64-QAM constellations, respectively:  $15^\circ, 8.5^\circ$ , and  $4.5^\circ$ .

#### IV. SIMULATION RESULTS

In this section, simulation results are presented for the CI-OFDM-IM, OFDM-IM and OFDM schemes assuming the following system parameters:  $N_F = 128, C_p = 16, L = 10$ .

In Fig. 2, we compare the uncoded and coded BER performances of OFDM, OFDM-IM and CI-OFDM-IM, where ML detection with the look-up table given in Table I and block interleavers are used for 4-QAM. The rate-1/3 LTE convolutional code (CC) is considered for the coded transmission [9]. As seen from Fig. 2, significant BER performance improvements can be obtained by the CI-OFDM scheme for both uncoded and

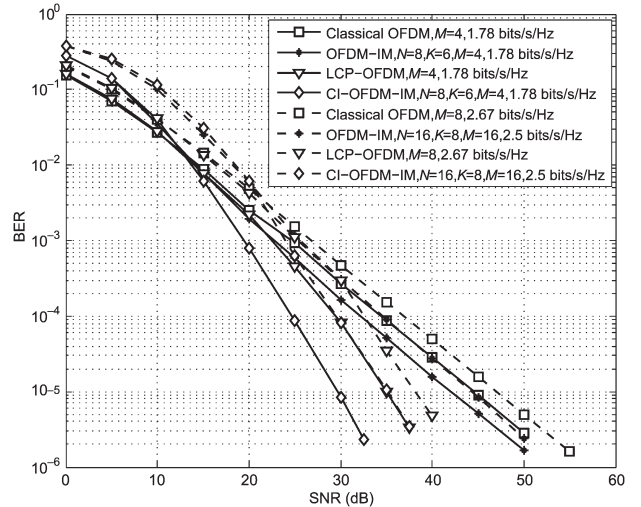


Fig. 3. Performance of OFDM, OFDM-IM, LCP-OFDM and CI-OFDM-IM.

coded cases, due to its higher diversity order. We also observe from Fig. 2, that the theoretical ABEP upper bound exhibits reasonable results with the increasing SNR.

In Fig. 3, we compare the BER performance of the OFDM, OFDM-IM, linear constellation precoding OFDM (LCP-OFDM) [10] and CI-OFDM-IM schemes for two different spectral efficiency values. As seen from Fig. 3, significant BER performance improvements can be achieved by the CI-OFDM-IM scheme compared to the reference systems.

#### V. CONCLUSION

A novel OFDM scheme called CI-OFDM-IM, which combines OFDM-IM and coordinate interleaving has been proposed in this letter. By the use of coordinate interleaving, a diversity gain has been obtained for the OFDM-IM scheme.

#### REFERENCES

- [1] E. Başar, Ü Aygözü, E. Panayirci, and H. V. Poor, "Orthogonal frequency division multiplexing with index modulation," *IEEE Trans. Signal Process.*, vol. 61, no. 22, pp. 5536–5549, Nov. 2013.
- [2] Y. Xiao *et al.*, "OFDM with interleaved subcarrier-index modulation," *IEEE Commun. Lett.*, vol. 18, no. 8, pp. 1447–1450, Aug. 2014.
- [3] Y. Ko, "A tight upper bound on bit error rate of joint OFDM and multi-carrier index keying," *IEEE Commun. Lett.*, vol. 18, no. 10, pp. 1763–1766, Oct. 2014.
- [4] R. Fan, Y. J. Yu, and Y. L. Guan, "Orthogonal frequency division multiplexing with generalized index modulation," in *Proc. IEEE Global Commun. Conf.*, Dec. 2014, pp. 3880–3885.
- [5] M. Wen, X. Cheng, and L. Yang, "Optimizing the energy efficiency of OFDM with index modulation," in *Proc. IEEE Int. Conf. Commun. Syst.*, Nov. 2014, pp. 31–35.
- [6] M. Z. A. Khan and B. S. Rajan, "Single-symbol maximum likelihood decodable linear STBCs," *IEEE Trans. Inf. Theory*, vol. 52, no. 5, pp. 2062–2091, May 2006.
- [7] X. Guo and X.-G. Xia, "On full diversity space-time block codes with partial interference cancellation group decoding," *IEEE Trans. Inf. Theory*, vol. 55, no. 10, pp. 4366–4385, Oct. 2009.
- [8] M. Simon and M. S. Alouini, *Digital Communications Over Fading Channels*. New York, NY, USA: Wiley, 2005.
- [9] S. Ahmadi, *LTE-Advanced A Practical Systems Approach to Understanding the 3GPP LTE Releases 10 and 11 Radio Access Technologies*. New York, NY, USA: Academic, 2014.
- [10] Z. Liu, Y. Xin, and G. Giannakis, "Linear constellation precoding for OFDM with maximum multipath diversity and coding gains," *IEEE Trans. Commun.*, vol. 51, no. 3, pp. 416–427, Mar. 2003.